$\pi^{\pm}p$ Elastic Scattering in the 2-GeV Region

W. Busza,* B. G. Duff, D. A. Garbutt,† F. F. Heymann, C. C. Nimmon, K. M. Potter,‡ and T. P. Swetman
University College, London, England

AND

E. H. Bellamy, T. F. Buckley, R. W. Dobinson,§ P. V. March, J. A. Strong, and R. N. F. Walker
Westfield College, London, England

(Received 18 October 1968)

$\pi^{\pm}p$ elastic differential cross sections in the momentum range 1.72–2.80 GeV/c have been measured at the proton synchrotron "NIMROD" of the Rutherford High Energy Laboratory. The results are tabulated, and analyses of the differential cross sections employing optical models and Legendre polynomial expansions are advanced. A critical discussion of a recent interpretation of differential-cross-section structure in terms of interference between resonant and background amplitudes is presented.

1. INTRODUCTION

THIS paper presents the results of a series of pion-proton elastic differential cross-section measurements in the range 1.72–2.80 GeV/c pion laboratory momentum. The experiments were performed at the 7-GeV/c proton synchrotron "NIMROD" of the Rutherford High Energy Laboratory. The beam, hydrogen target, and spark-chamber detection system were essentially the same as those described previously[1,2]; however, a modified scintillation-counter and spark-chamber system was used to provide improved inelastic rejection and greater accuracy in track location (see Fig. 1). Data were taken at the following fifteen pion laboratory momenta:

π^+p: 1.72, 1.89, 2.07, 2.17, 2.27, 2.36, 2.46, 2.56, 2.65, and 2.80 GeV/c;

π^-p: 2.17, 2.36, 2.56, 2.65, and 2.80 GeV/c.

π^-p data at 1.72, 1.89, 2.07, 2.27, and 2.46 GeV/c, previously reported elsewhere,[2,3] are included here for completeness.

2. DATA REDUCTION

The film data were scanned and measured on D-MAC digitized track measuring machines, and analyzed with the aid of the Atlas computer of the University of London Computing Centre. Final selection of elastic events was made by imposing severe coplanarity and kinematic constraints.[4] The data were corrected to take account of the inelastic and target empty backgrounds, the geometrical detection efficiency, the pion-proton kinematical cross-over region, and scanning inefficiencies. The ten π^-p angular distributions were normalized to the zero-degree cross-section values of Höhler *et al.*[5] by exponential extrapolation of the diffraction-peak data [i.e., data satisfying $0<|t|\leq 0.4$ (GeV/c)^2, t=squared four-momentum transfer]. Absolute values of the ten π^+p differential cross sections (dcs) were obtained by applying corrections for muon and electron beam contamination, and event losses in analysis. The absolute π^+p dcs, and the π^-p dcs, normalized as described above, are presented in Tables I and II, respectively. The errors quoted are statistical only.

Table III presents a comparison of the absolute π^+p dcs, extrapolated to zero degrees, with the forward dcs predictions of Höhler *et al.*[5] The close agreement illustrates the accuracy of the correction procedures applied to the π^+p data.

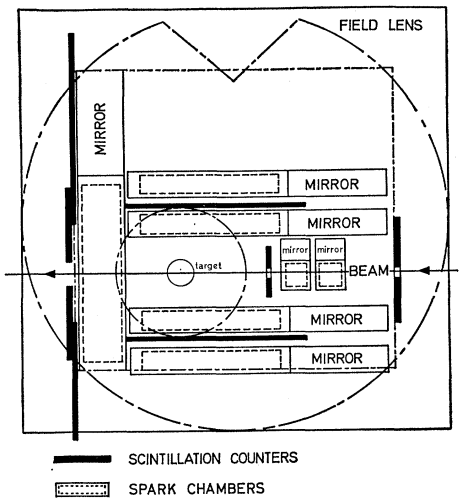

FIG. 1. Experimental apparatus (plan). Diameter of field lens is 4 ft.

* Present address: Stanford Linear Accelerator Center, Stanford University, Stanford, Calif.
† Present address: Physics Department, Imperial College, London, England.
‡ Imperial Chemical Industries Research Fellow in the University of London.
§ Present address: CERN, Geneva, Switzerland.
[1] E. H. Bellamy *et al.*, Proc. Roy. Soc. (London) **289**, 509 (1965).
[2] W. Busza *et al.*, Rutherford High Energy Laboratory Report No. RPP/H/21, 1966 (unpublished).
[3] W. Busza *et al.*, Nuovo Cimento **52A**, 331 (1967).
[4] K. M. Potter, Thesis, University College London, 1967 (unpublished).
[5] G. Höhler *et al.*, Z. Physik **180**, 430 (1964); private communication, via R. W. Dobinson, 1967.

TABLE I. π^+p differential cross section.

cos θ	Cross section (mb/sr)
Pion lab momentum 1.72 GeV/c.	
0.95[a]	5.78 ±0.38
0.93	6.87 ±0.43
0.91	6.57 ±0.42
0.89	5.01 ±0.33
0.87	4.82 ±0.35
0.85	3.88 ±0.30
0.83	3.50 ±0.29
0.81	2.25 ±0.20
0.79	2.21 ±0.21
0.76	1.44 ±0.11
0.72	0.934±0.092
0.68	0.536±0.068
0.64	0.315±0.048
0.60	0.199±0.041
0.55	0.144±0.030
0.49	0.092±0.027
0.43	0.140±0.036
0.37	0.154±0.044
0.31	0.240±0.054
0.17	0.229±0.024
0.03	0.364±0.067
−0.03	0.444±0.069
−0.09	0.456±0.066
−0.15	0.400±0.052
−0.21	0.455±0.056
−0.27	0.511±0.058
−0.33	0.522±0.061
−0.39	0.470±0.055
−0.45	0.586±0.063
−0.52	0.568±0.057
−0.60	0.575±0.055
−0.68	0.411±0.043
−0.76	0.290±0.036
−0.84	0.182±0.027
−0.90	0.199±0.043
−0.94	0.208±0.055
Pion lab momentum 1.89 GeV/c.	
0.93	6.35 ±0.43
0.91	5.19 ±0.37
0.89	4.54 ±0.33
0.87	4.80 ±0.37
0.85	3.34 ±0.28
0.83	2.69 ±0.25
0.81	2.08 ±0.21
0.79	2.05 ±0.21
0.76	1.30 ±0.11
0.72	1.06 ±0.10
0.68	0.584±0.076
0.64	0.328±0.053
0.59	0.232±0.041
0.53	0.108±0.031
0.47	0.105±0.034
0.41	0.222±0.056
0.35	0.279±0.066
0.29	0.239±0.063
0.16	0.216±0.026
0.03	0.128±0.050
−0.03	0.263±0.058
−0.09	0.255±0.052
−0.15	0.188±0.038
−0.21	0.193±0.038
−0.27	0.265±0.045
−0.33	0.241±0.042
−0.39	0.296±0.046
−0.45	0.198±0.038
−0.52	0.268±0.040
−0.60	0.167±0.032
−0.68	0.169±0.031
−0.76	0.067±0.021
−0.84	0.048±0.019
−0.90	0.034±0.026
−0.94	0.035±0.037
Pion lab momentum 2.07 GeV/c	
0.95	6.43 ±0.42
0.93	5.75 ±0.36
0.91	4.72 ±0.31
0.89	4.40 ±0.29
0.87	4.08 ±0.29
0.85	3.05 ±0.24
0.83	2.27 ±0.20
0.81	1.86 ±0.17
0.78	1.31 ±0.09
0.74	0.990±0.087
0.70	0.629±0.070
0.66	0.374±0.049
0.62	0.280±0.044
0.58	0.226±0.042
0.53	0.186±0.032
0.47	0.142±0.033
0.41	0.141±0.040
0.35	0.151±0.042
0.29	0.099±0.039
0.15	0.159±0.018
0.01	0.146±0.042
−0.05	0.138±0.036
−0.11	0.186±0.038
−0.17	0.158±0.030
−0.23	0.150±0.027
−0.29	0.122±0.025
−0.35	0.155±0.027
−0.41	0.170±0.028
−0.47	0.120±0.024
−0.53	0.112±0.025
−0.60	0.079±0.018
−0.68	0.071±0.017
−0.76	0.052±0.015
−0.84	0.028±0.012
−0.90	0.030±0.018
−0.94	0.040±0.027
Pion lab momentum 2.17 GeV/c	
0.95	6.28 ±0.58
0.93	5.72 ±0.51
0.91	5.13 ±0.46
0.89	4.52 ±0.41
0.87	3.64 ±0.38
0.85	2.67 ±0.32
0.83	2.11 ±0.28
0.81	2.31 ±0.28
0.78	1.35 ±0.15
0.74	0.575±0.097
0.70	0.507±0.089
0.66	0.392±0.079
0.62	0.310±0.074
0.58	0.137±0.052
0.53	0.110±0.043
0.47	0.188±0.058
0.41	0.152±0.074
0.35	0.121±0.066
0.29	0.371±0.108
0.15	0.134±0.029
0.01	0.132±0.077
−0.05	0.120±0.057
−0.11	0.155±0.061
−0.17	0.068±0.035
−0.23	0.086±0.036
−0.29	0.115±0.041
−0.35	0.044±0.028
−0.41	0.117±0.040
−0.47	0.109±0.040
−0.53	0.016±0.026
−0.60	0.038±0.027
−0.68	0.046±0.027
−0.76	0.045±0.028
−0.84	0.087±0.032
−0.90	0.077±0.045
−0.94	0.024±0.045
Pion lab momentum 2.27 GeV/c	
0.95	7.32 ±0.47
0.93	6.52 ±0.40
0.91	5.28 ±0.34
0.89	4.33 ±0.29
0.87	3.38 ±0.27
0.85	2.77 ±0.24
0.83	2.23 ±0.21
0.81	1.87 ±0.18
0.78	1.21 ±0.11
0.74	0.755±0.083
0.70	0.575±0.071
0.66	0.219±0.043
0.62	0.170±0.041
0.57	0.161±0.035
0.51	0.118±0.031
0.45	0.178±0.045
0.39	0.245±0.062
0.33	0.278±0.067
0.27	0.243±0.069
0.14	0.139±0.068
0.01	0.051±0.052
−0.05	0.047±0.036
−0.11	0.054±0.036
−0.17	0.075±0.031
−0.23	0.069±0.025
−0.29	0.067±0.024
−0.35	0.106±0.028
−0.41	0.040±0.025
−0.47	0.060±0.024
−0.53	0.043±0.038
−0.60	0.002±0.015
−0.68	−0.021±0.013
−0.76	0.018±0.016
−0.84	0.015±0.015
−0.90	0.074±0.031
−0.94	0.059±0.038
Pion lab momentum 2.36 GeV/c	
0.95	6.32 ±0.69
0.93	6.21 ±0.61
0.91	4.65 ±0.53
0.89	3.59 ±0.40
0.87	3.29 ±0.41
0.85	2.47 ±0.35
0.83	1.93 ±0.30
0.81	1.51 ±0.26
0.78	0.890±0.140
0.74	0.440±0.100
0.70	0.370±0.093
0.66	0.217±0.071
0.62	0.137±0.061
0.57	0.142±0.053
0.51	0.121±0.051
0.45	0.190±0.084
0.39	0.147±0.084
0.33	0.120±0.084
0.27	0.099±0.078
0.13	0.200±0.040
−0.01	0.037±0.071
−0.07	0.116±0.084
−0.13	0.031±0.056
−0.19	0.079±0.051
−0.25	0.043±0.039
−0.31	0.073±0.045
−0.40	0.002±0.022
−0.49	0.055±0.038
−0.55	0.087±0.052
−0.61	0.017±0.035
−0.68	0.023±0.031
−0.76	0.085±0.038
−0.84	0.071±0.036
−0.90	0.082±0.056
−0.94	0.097±0.093
Pion lab momentum 2.46 GeV/c	
0.95	7.63 ±0.47
0.93	6.73 ±0.40
0.91	5.08 ±0.32
0.89	3.72 ±0.26
0.87	2.86 ±0.23
0.85	2.38 ±0.21
0.83	1.75 ±0.18
0.81	1.39 ±0.15
0.78	0.813±0.081
0.74	0.583±0.069
0.70	0.345±0.053
0.66	0.167±0.038
0.61	0.115±0.028
0.55	0.134±0.031
0.49	0.118±0.031
0.43	0.147±0.043
0.37	0.201±0.048
0.31	0.176±0.047
0.25	0.114±0.038
0.12	0.119±0.017
−0.01	0.053±0.036
−0.07	0.071±0.036
−0.13	0.053±0.032
−0.19	0.021±0.024
−0.25	0.011±0.017
−0.31	0.037±0.019
−0.37	0.024±0.018
−0.43	0.031±0.017
−0.49	0.039±0.020
−0.56	0.043±0.018
−0.64	0.059±0.019
−0.72	0.049±0.016
−0.80	0.034±0.014
−0.86	0.070±0.028
−0.90	0.100±0.034
−0.94	0.038±0.039
Pion lab momentum 2.56 GeV/c	
0.95	7.77 ±0.75
0.93	5.81 ±0.57

TABLE I (*continued*)

$\cos\theta$	Cross section (mb/sr)	$\cos\theta$	Cross section (mb/sr)	$\cos\theta$	Cross section (mb/sr)	$\cos\theta$	Cross section (mb/sr)
Pion lab momentum 2.56 GeV/c		Pion lab momentum 2.56 GeV/c		Pion lab momentum 2.65 GeV/c		Pion lab momentum 2.80 GeV/c	
0.91	4.85 ±0.48	−0.84	0.098±0.036	−0.09	0.047±0.039	0.70	0.155±0.039
0.89	3.60 ±0.43	−0.90	0.137±0.064	−0.15	0.021±0.030	0.66	0.187±0.043
0.87	2.63 ±0.34	−0.94	0.076±0.075	−0.21	0.035±0.028	0.62	0.094±0.034
0.85	2.30 ±0.32			−0.27	0.003±0.018	0.57	0.136±0.034
0.83	2.00 ±0.29	Pion lab momentum 2.65 GeV/c		−0.33	0.027±0.020	0.51	0.162±0.026
0.81	1.23 ±0.22			−0.39	0.022±0.018	0.45	0.168±0.053
0.78	0.867±0.130			−0.45	0.036±0.020	0.39	0.154±0.050
0.74	0.381±0.092	0.95	7.72 ±0.51	−0.52	0.008±0.015	0.33	0.156±0.049
0.70	0.166±0.059	0.93	6.69 ±0.43	−0.60	0.020±0.017	0.27	0.060±0.040
0.66	0.073±0.046	0.91	5.44 ±0.35	−0.68	0.037±0.018	0.13	0.067±0.015
0.61	0.098±0.040	0.89	3.53 ±0.26	−0.76	0.050±0.022	−0.01	0.043±0.037
0.55	0.138±0.051	0.87	2.98 ±0.25	−0.84	0.050±0.021	−0.07	0.065±0.040
0.49	0.121±0.050	0.85	1.82 ±0.18	−0.90	0.081±0.034	−0.13	0.033±0.037
0.43	0.223±0.083	0.83	1.42 ±0.16	−0.94	0.052±0.042	−0.19	0.034±0.032
0.37	0.294±0.092	0.81	1.14 ±0.14			−0.25	0.006±0.026
0.31	0.150±0.072	0.78	0.663±0.076			−0.31	0.056±0.030
0.25	0.228±0.083	0.74	0.328±0.055	Pion lab momentum 2.80 GeV/c		−0.37	0.033±0.022
0.11	0.133±0.028	0.70	0.174±0.040			−0.43	0.031±0.018
−0.03	0.042±0.061	0.66	0.122±0.034	0.95	8.08 ±0.57	−0.49	0.072±0.026
−0.09	0.057±0.062	0.61	0.174±0.034	0.93	6.30 ±0.43	−0.55	0.037±0.022
−0.15	0.021±0.045	0.55	0.125±0.033	0.91	5.37 ±0.37	−0.61	0.043±0.024
−0.24	0.018±0.025	0.49	0.104±0.031	0.89	3.32 ±0.26	−0.68	0.036±0.018
−0.33	0.077±0.041	0.43	0.130±0.042	0.87	3.08 ±0.27	−0.76	0.102±0.026
−0.39	0.051±0.034	0.37	0.112±0.040	0.85	1.81 ±0.19	−0.84	0.067±0.022
−0.49	0.003±0.017	0.31	0.130±0.044	0.83	1.41 ±0.17	−0.90	0.015±0.030
−0.60	0.024+0.028	0.25	0.086±0.038	0.81	0.812±0.130	−0.94	0.047±0.040
−0.68	0.050±0.030	0.11	0.096±0.017	0.78	0.640±0.079		
−0.76	0.113±0.040	−0.03	0.025±0.032	0.74	0.347±0.059		

[a] Subject to approximately 20% correction for loss of recoil protons.

3. INTERPRETATIONS OF DIFFERENTIAL CROSS SECTIONS

A. Legendre Polynomial Expansions

The differential cross sections of Table I and II have been fitted with the Legendre polynomial expansions

$$\frac{d\sigma}{d\Omega}=\lambda^2\sum_{n=0}^{N\max}C_nP_n(\cos\theta). \quad (1)$$

The resulting Legendre polynomial coefficients C_n are plotted in Figs. 2 and 3 for π^+p and π^-p data, respectively.

The π^+p C_n coefficients, combined with π^-p dcs[2,3] and polarization data,[6] and information from 180° π^+p dcs measurements[7] have been used in an attempt to establish the spin and parity of the $\Delta(2420)$ as $\frac{11}{2}^+$.[8] The coefficients D_n in the associated Legendre expansion for π^-p elastic scattering, exhibited in Fig. 2 of Ref. 8, were quantitatively incorrect. Correct values of the coefficients are given in Table IV of the present publication. The conclusions of Ref. 8 regarding the J^P assignment of the $\Delta(2420)$ remain unaltered. Quantitative fitting of the π^-p C_n coefficients has also provided evidence for the $\frac{7}{2}^-$ assignment of the $N(2190)$.[3] The additional π^-p data presented in this paper support the conclusions of this earlier work.

[6] A. Yokosawa *et al.*, Phys. Rev. Letters **16**, 714 (1966).
[7] T. Dobrowolski *et al.*, Phys. Letters **24B**, 203 (1967).
[8] E. H. Bellamy *et al.*, Phys. Rev. Letters **19**, 476 (1967).

B. Exponential Behavior of the Diffraction Peak

Following the original suggestion by Damouth *et al.*,[9] many authors have attempted to obtain information on baryon resonances from the behavior of the dcs in the diffraction-peak region.[10] The present data have been fitted with the exponential expression,

$$\frac{d\sigma}{d\Omega}=\left(\frac{d\sigma}{d\Omega}\right)_0 e^{At}, \quad (2)$$

in the region $0<|t|\leq 0.4$ (GeV/c)^2. The A coefficients from these fits, combined with earlier data,[9,10] are shown in Figs. 4 and 5, and listed in Table V. Considerable structure is apparent, particularly in the π^+p data at center-of-mass energies of approximately 1920 and 2420 MeV. The positions of the known πN resonances are indicated.

C. Optical Models

The data have been fitted with various optical models, using a minimization routine developed by Powell.[11]

[9] D. E. Damouth *et al.*, Phys. Rev. Letters **11**, 287 (1963).
[10] N. M. Gelfand *et al.*, Phys. Rev. Letters **17**, 1224 (1966); R. Levi-Setti and E. Predazzi, in *Proceedings of the Thirteenth International Conference on High-Energy Physics, Berkeley, California, 1966* (University of California Press, Berkeley, 1967); L. D. Jacobs, University of California Radiation Laboratory Report No. UCRL 16877 (unpublished).
[11] M. J. D. Powell, Computer J. **7**, 155 (1964).

TABLE II. $\pi^- p$ differential cross section.

$\cos\theta$	Cross section (mb/sr)
Pion lab momentum 1.72 GeV/c	
0.93	6.07 ±0.51
0.91	5.91 ±0.50
0.89	4.78 ±0.44
0.87	3.82 ±0.41
0.85	2.84 ±0.34
0.83	2.70 ±0.35
0.81	3.32 ±0.39
0.79	2.07 ±0.28
0.77	1.72 ±0.26
0.75	1.33 ±0.24
0.73	0.488±0.15
0.71	1.00 ±0.22
0.69	0.636±0.181
0.67	0.524±0.169
0.64	0.243±0.099
0.58	0.160±0.058
0.50	0.104±0.041
0.42	0.104±0.042
0.34	0.104±0.044
0.22	0.131±0.033
0.06	0.119±0.056
−0.02	0.147±0.065
−0.10	0.118±0.043
−0.18	0.163±0.052
−0.26	0.187±0.048
−0.34	0.193±0.046
−0.42	0.247±0.052
−0.50	0.195±0.046
−0.58	0.130±0.040
−0.66	0.190±0.047
−0.74	0.083±0.034
−0.82	0.019±0.026
−0.90	0.007±0.026
Pion lab momentum 1.89 GeV/c	
0.93	7.49 ±0.55
0.91	6.37 ±0.48
0.89	4.73 ±0.37
0.87	4.58 ±0.39
0.85	3.61 ±0.36
0.83	2.70 ±0.30
0.81	1.81 ±0.26
0.79	2.16 ±0.24
0.77	1.77 ±0.26
0.75	1.22 ±0.21
0.73	1.46 ±0.23
0.71	0.527±0.177
0.69	0.915±0.223
0.66	0.306±0.114
0.62	0.134±0.094
0.56	0.067±0.041
0.48	0.086±0.039
0.40	0.156±0.044
0.32	0.218±0.046
0.24	0.340±0.073
0.16	0.216±0.042
0.10	0.227±0.132
0.04	0.042±0.052
−0.04	0.187±0.042
−0.12	0.151±0.040
−0.20	0.092±0.038
−0.28	0.146±0.040
−0.36	0.088±0.028
−0.44	0.088±0.031
−0.52	0.103±0.033
−0.60	0.077±0.030
−0.68	0.024±0.024
−0.76	0.024±0.023
−0.84	0.014±0.025
−0.92	0.029±0.034

$\cos\theta$	Cross section (mb/sr)
Pion lab momentum 2.07 GeV/c	
0.93	6.54 ±0.50
0.91	5.00 ±0.42
0.89	4.20 ±0.34
0.87	2.53 ±0.29
0.85	2.61 ±0.30
0.83	1.57 ±0.23
0.81	1.15 ±0.21
0.79	1.18 ±0.18
0.77	0.907±0.189
0.75	0.556±0.150
0.73	0.360±0.131
0.71	0.324±0.145
0.68	0.315±0.105
0.64	0.046±0.062
0.56	0.065±0.038
0.48	0.036±0.031
0.40	0.107±0.038
0.32	0.137±0.045
0.24	0.173±0.059
0.16	0.209±0.036
0.05	0.232±0.053
−0.04	0.110±0.034
−0.12	0.106±0.032
−0.20	0.063±0.031
−0.28	0.077±0.030
−0.36	0.059±0.023
−0.44	0.050±0.028
−0.52	0.024±0.024
−0.60	0.015±0.019
−0.68	0.007±0.018
=0.76	0.009±0.020
−0.84	0.017±0.025
−0.92	0.052±0.035
Pion lab momentum 2.17 GeV/c	
0.93	6.84 ±0.78
0.91	4.82 ±0.62
0.89	4.05 ±0.54
0.87	3.57 ±0.54
0.85	2.69 ±0.46
0.83	1.69 ±0.36
0.81	1.54 ±0.33
0.79	0.928±0.261
0.77	0.446±0.186
0.75	0.283±0.149
0.73	0.259±0.150
0.70	0.353±0.113
0.67	0.095±0.099
0.65	0.083±0.080
0.62	0.090±0.065
0.58	0.033±0.063
0.53	0.057±0.054
0.44	0.134±0.065
0.32	0.101±0.079
0.15	0.127±0.048
0.01	0.103±0.126
−0.05	0.240±0.126
−0.11	0.096±0.104
−0.20	0.030±0.047
−0.32	0.024±0.020
−0.44	0.002±0.035
−0.53	0.063±0.067
−0.64	0.034±0.040
−0.76	0.017±0.047
−0.84	0.096±0.049
−0.92	0.095±0.073
Pion lab momentum 2.27 GeV/c	
0.93	6.03 ±0.44

$\cos\theta$	Cross section (mb/sr)
Pion lab momentum 2.27 GeV/c	
0.91	6.02 ±0.43
0.89	3.58 ±0.32
0.87	3.28 ±0.31
0.85	2.22 ±0.25
0.83	1.65 ±0.24
0.81	1.42 ±0.25
0.79	0.711±0.150
0.77	0.639±0.141
0.75	0.359±0.123
0.73	0.421±0.126
0.70	0.136±0.071
0.66	0.039±0.060
0.62	0.041±0.049
0.54	0.037±0.034
0.46	0.121±0.039
0.38	0.143±0.035
0.30	0.233±0.046
0.22	0.252±0.060
0.14	0.196±0.038
0.06	0.132±0.060
−0.02	0.084±0.035
−0.10	0.093±0.029
−0.18	0.037±0.023
−0.26	0.065±0.027
−0.34	0.044±0.021
−0.42	0.013±0.016
−0.50	0.044±0.022
−0.58	0.009±0.016
−0.66	0.024±0.019
−0.74	0.001±0.015
−0.82	0.080±0.028
−0.90	0.086±0.032
Pion lab momentum 2.36 GeV/c	
0.95	6.70 ±0.79
0.93	6.40 ±0.68
0.90	4.94 ±0.43
0.87	3.14 ±0.44
0.85	1.96 ±0.34
0.83	1.53 ±0.30
0.81	1.01 ±0.23
0.79	0.932±0.225
0.77	0.392±0.149
0.75	0.182±0.102
0.73	0.264±0.123
0.71	0.309±0.127
0.69	0.214±0.105
0.67	0.088±0.075
0.65	0.158±0.087
0.62	0.024±0.044
0.57	0.072±0.043
0.51	0.130±0.058
0.45	0.113±0.084
0.39	0.182±0.099
0.33	0.177±0.102
0.27	0.142±0.112
0.13	0.106±0.034
−0.01	0.219±0.124
−0.07	0.095±0.080
−0.13	0.155±0.082
−0.19	0.086±0.061
−0.25	0.066±0.051
−0.34	0.010±0.030
−0.43	0.015±0.033
−0.49	0.009±0.033
−0.55	0.009±0.040
−0.61	0.016±0.037
−0.68	0.073±0.040
−0.76	0.046±0.036
−0.84	0.135±0.050

$\cos\theta$	Cross section (mb/sr)
Pion lab momentum 2.36 GeV/c	
−0.90	0.125±0.075
−0.94	0.058±0.101
Pion lab momentum 2.46 GeV/c	
0.93	6.81 ±0.49
0.91	4.21 ±0.38
0.89	3.35 ±0.33
0.87	2.81 ±0.30
0.85	1.74 ±0.23
0.83	1.59 ±0.24
0.81	0.968±0.205
0.79	0.664±0.146
0.77	0.467±0.129
0.70	0.056±0.067
0.66	0.034±0.066
0.62	0.009±0.043
0.54	0.034±0.030
0.46	0.119±0.036
0.38	0.061±0.031
0.30	0.077±0.037
0.22	0.159±0.052
0.10	0.064±0.025
−0.02	0.086±0.033
−0.10	0.044±0.023
−0.18	0.027±0.020
−0.26	0.026±0.022
−0.34	0.006±0.017
−0.42	0.006±0.017
−0.50	0.022±0.017
−0.58	0.029±0.019
−0.66	0.017±0.017
−0.74	0.018±0.017
−0.82	0.015±0.019
−0.90	0.030±0.026
Pion lab momentum 2.56 GeV/c	
0.95	9.03 ±0.80
0.93	7.57 ±0.65
0.91	5.62 ±0.51
0.89	3.41 ±0.36
0.87	3.59 ±0.39
0.85	2.43 ±0.31
0.83	1.58 ±0.25
0.81	1.31 ±0.22
0.79	0.553±0.143
0.76	0.484±0.092
0.72	0.227±0.066
0.68	0.102±0.046
0.65	0.042±0.042
0.61	0.101±0.037
0.55	0.101±0.042
0.49	0.180±0.055
0.40	0.135±0.040
0.31	0.115±0.056
0.25	0.108±0.053
0.11	0.127±0.025
0.03	0.104±0.055
−0.09	0.089±0.058
−0.20	0.020±0.010
−0.46	0.001±0.009
−0.78	0.002±0.012
−0.90	0.051±0.040
−0.94	0.111±0.061
Pion lab momentum 2.65 GeV/c	
0.95	8.37 ±0.55
0.93	6.70 ±0.43

TABLE II (*continued*)

$\cos\theta$	Cross section (mb/sr)	$\cos\theta$	Cross section (mb/sr)	$\cos\theta$	Cross section (mb/sr)	$\cos\theta$	Cross section (mb/sr)
Pion lab momentum 2.65 GeV/c		Pion lab momentum 2.65 GeV/c		Pion lab momentum 2.80 GeV/c		Pion lab momentum 2.80 GeV/c	
0.91	4.59 ±0.31	0.31	0.130±0.035	0.93	6.97 ±0.45	0.45	0.076±0.027
0.89	3.42 ±0.24	0.25	0.071±0.028	0.91	5.06 ±0.34	0.39	0.096±0.030
0.87	2.56 ±0.21	0.11	0.081±0.013	0.89	3.46 ±0.25	0.33	0.065±0.026
0.85	1.59 ±0.16	−0.03	0.078±0.029	0.87	2.38 ±0.21	0.27	0.079±0.031
0.83	1.30 ±0.14	−0.09	0.049±0.026	0.85	1.66 ±0.17	0.13	0.049±0.010
0.81	0.956±0.114	−0.15	0.042±0.022	0.83	1.20 ±0.14	−0.01	0.036±0.024
0.79	0.537±0.084	−0.21	0.019±0.017	0.81	0.723±0.099	−0.07	0.049±0.022
0.77	0.442±0.075	−0.30	0.006±0.008	0.79	0.585±0.090	−0.13	0.077±0.027
0.75	0.267±0.058	−0.39	0.006±0.010	0.77	0.333±0.067	−0.19	0.021±0.015
0.73	0.215±0.054	−0.49	0.001±0.006	0.75	0.203±0.053	−0.25	0.014±0.012
0.71	0.120±0.040	−0.64	0.003±0.006	0.73	0.144±0.047	−0.31	0.013±0.012
0.69	0.154±0.044	−0.76	0.018±0.011	0.71	0.092±0.038	−0.40	0.007±0.007
0.67	0.099±0.039	−0.84	0.025±0.012	0.69	0.149±0.045	−0.49	0.016±0.012
0.65	0.046±0.024	−0.90	0.015±0.021	0.67	0.115±0.043	−0.55	0.001±0.011
0.61	0.088±0.021	−0.94	−0.087±0.020	0.65	0.069±0.031	−0.61	0.015±0.013
0.55	0.085±0.023			0.63	0.044±0.027	−0.72	0.010±0.006
0.49	0.097±0.025	Pion lab momentum 2.80 GeV/c		0.61	0.124±0.044	−0.84	0.043±0.014
0.43	0.186±0.042			0.57	0.085±0.024	−0.90	0.055±0.026
0.37	0.126±0.034	0.95	7.88 ±0.54	0.51	0.116±0.029	−0.94	−0.002±0.034

Two-Parameter Gray-Disk Model

In this model,[12] the dcs is parametrized in terms of an "interaction radius" R, and an opacity a

$$d\sigma/d\Omega=(1-a)^2R^2[J_1(2kR\sin\tfrac{1}{2}\theta)/2\sin\tfrac{1}{2}\theta]^2. \quad (3)$$

Best-fit values of R and a obtained with the present π^+p cross-section data are given in Table VI.

Empirical Partial-Wave Analysis

Data at all momenta have been fitted with the spin-independent purely absorptive partial-wave expansions:

$$\frac{d\sigma}{d\Omega}=\left|(2ik)^{-1}\sum_{l=0}^{L\max}(2l+1)a_lP_l(\cos\theta)\right|^2. \quad (4)$$

The absorption parameters a_l were subjected to the constraints

$$0\leq a_l\leq 1.0, \quad l\geq 1;$$
$$0\leq a_l\leq 2.0, \quad l=0.$$

The best-fit values of a_l are given in Table VII (π^+ data only). These results are in good qualitative agreement with those obtained by Perl and Corey,[13] the a_l being smoothly varying functions of l. A typical fit to the data is shown in Fig. 6 (π^+p, 2.46 GeV/c).

The data have also been fitted with the spin-dependent purely absorptive partial-wave expansions; however, inclusion of the spin-flip terms did not result in any improvement in the quality of the fit.

[12] R. J. Glauber, *Lectures in Theoretical Physics at the University of Colorado* (Wiley-Interscience, Inc., New York, 1959).
[13] M. L. Perl and M. C. Corey, Phys. Rev. **136**, B787 (1964).

D. Secondary Maxima in πp dcs

Hoff[14] has suggested that the dip at $t\sim -0.6$ (GeV/c)^2 and the secondary maximum in the π^-p elastic dcs in the region of 2 GeV are purely resonance phenomena. A calculation of the type used by Hoff has been made using dcs from the present experiment at 1.89, 2.07, and 2.27 GeV/c, and the results indicate that such calculations are very sensitive to the values chosen for the width and mass of the resonance.

Using the nomenclature of Ref. 14

$$\frac{d\sigma}{d\Omega}=\left(\frac{d\sigma}{d\Omega}\right)_b+\left(\frac{d\sigma}{d\Omega}\right)_i+\left(\frac{d\sigma}{d\Omega}\right)_r, \quad (5)$$

$$k^2\left(\frac{d\sigma}{d\Omega}\right)_b=\left(k^2\frac{d\sigma}{d\Omega}\right)_{\delta l=\pi/4}+\left(k^2\frac{d\sigma}{d\Omega}\right)_{\delta l=3\pi/4}-\left(k^2\frac{d\sigma}{d\Omega}\right)_{\delta l=\pi/2}, \quad (6)$$

TABLE III. Comparison of absolute π^+p differential cross sections, extrapolated to zero degrees, with results of Höhler *et al.* (Ref. 5).

Pion momentum (GeV/c)	$d\sigma/d\Omega(\theta=0)$ Extrapolation of present data (mb/sr)	$d\sigma/d\Omega(\theta=0)$ Höhler *et al.* (mb/sr)
1.72	15.4±1.2	12.9
1.89	12.0±1.0	11.8
2.07	11.3±0.8	11.9
2.17	10.2±0.7	12.6
2.27	13.2±0.6	13.7
2.36	12.6±1.2	14.9
2.46	15.3±0.8	16.1
2.56	14.1±0.9	17.0
2.65	18.0±1.7	17.6
2.80	17.5±2.1	18.2

[14] G. T. Hoff, Phys. Rev. Letters **18**, 816 (1967).

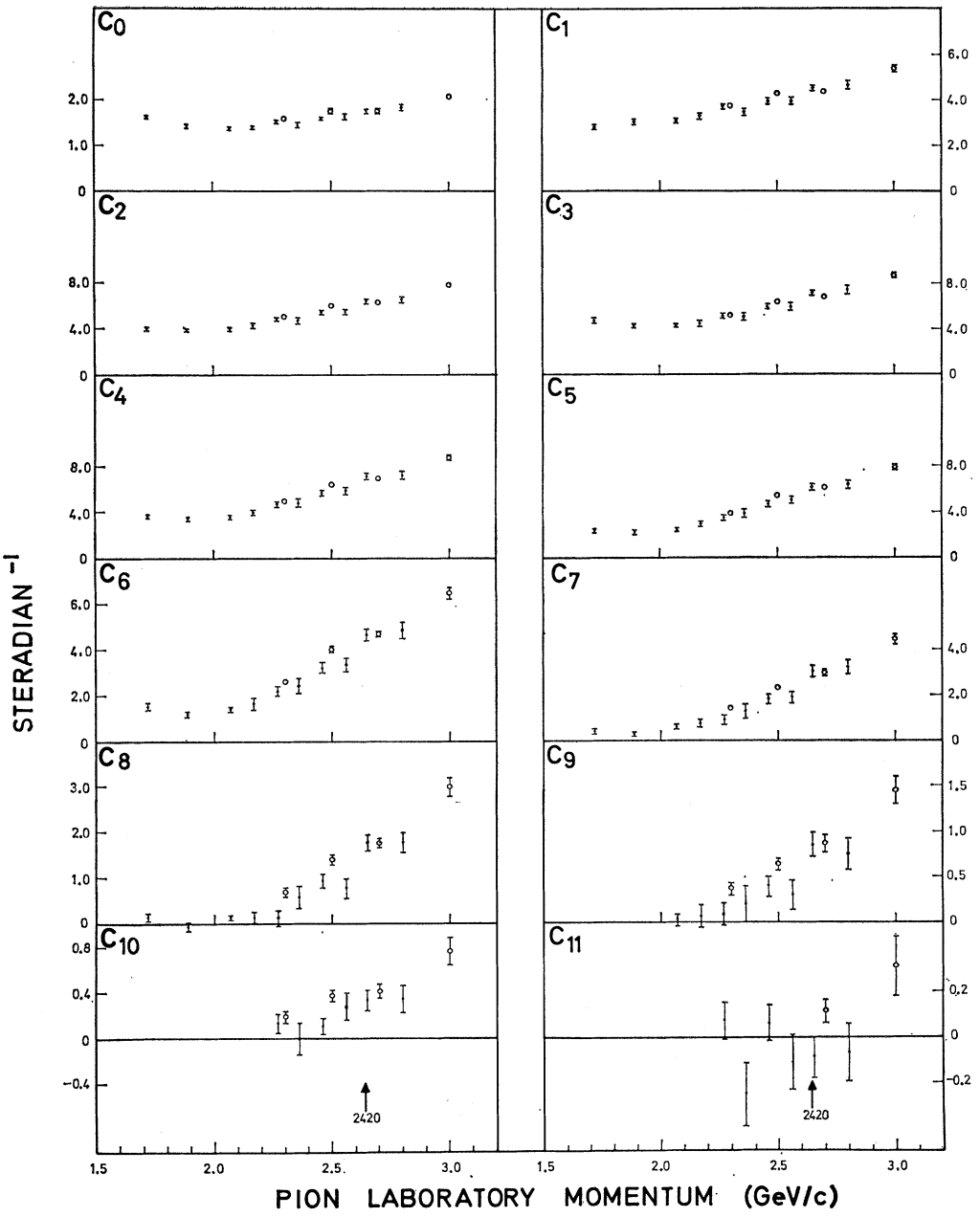

FIG. 2. π^+p: Legendre polynomial expansion coefficients. Open circles: data of C. T. Coffin *et al.*, [Phys. Rev. Letters **15**, 838 (1965)].

where the subscripts b, i, and r denote the background, interference, and resonance contributions to the dcs, respectively; δ_l is the eigenphase of the resonant contribution to the partial-wave amplitude of orbital angular momentum l, and k is the c.m. momentum. Equation (6) depends on the following assumptions: (a) If there is more that one resonant amplitude in this region, the resonant energies and total widths will be the same. (b) The magnitude of the background spin-nonflip and spin-flip amplitudes a_b and b_b, respectively, have a k^{-1} energy dependence at any fixed angle and their phases at a fixed angle may be assumed to be constant.

If the resonant amplitude can be satisfactorily described by a Breit-Wigner form, the relation between δ_l, the total width Γ_l, and the resonant energy $(\omega_R)_l$, is given by

$$\tan\delta_l=\Gamma_l/2[(\omega_R)_l-\omega]. \tag{7}$$

Taking a value of $\Gamma_l\sim200$ MeV for the $N(2190)$, as

TABLE IV. Coefficients (in sr^{-1}) in the associated Legendre expansion, $P(\theta)\frac{d\sigma}{d\Omega}=\lambda^2\sum_{1}^{N_{max}} D_n P_n^1(\cos\theta)$, for $\pi^- p$ elastic scattering.

	1.72 GeV/c	1.89 GeV/c	2.07 GeV/c	2.27 GeV/c	2.50 GeV/c	3.00 GeV/c
D1	−0.155±0.011	−0.228±0.011	−0.102 ±0.008	−0.094±0.027	−0.076±0.014	−0.168±0.042
D2	−0.079±0.011	−0.225±0.012	−0.073 ±0.006	−0.068±0.023	−0.089±0.013	−0.193±0.037
D3	−0.129±0.008	−0.256±0.015	−0.069 ±0.007	−0.047±0.012	−0.077±0.014	−0.173±0.045
D4	−0.183±0.010	−0.286±0.016	−0.102 ±0.008	−0.038±0.014	−0.069±0.016	−0.167±0.050
D5	−0.129±0.008	−0.248±0.014	−0.106 ±0.008	−0.053±0.015	−0.079±0.016	−0.187±0.051
D6	−0.084±0.006	−0.191±0.014	−0.082 ±0.006	−0.053±0.010	−0.089±0.014	−0.201±0.048
D7	−0.064±0.005	−0.133±0.011	−0.061 ±0.005	−0.052±0.009	−0.080±0.013	−0.183±0.042
D8	−0.024±0.004	−0.069±0.007	−0.038 ±0.004	−0.036±0.010	−0.058±0.011	−0.141±0.035
D9	(+0.003±0.004)	−0.025±0.006	−0.013 ±0.002	(+0.002±0.010)	−0.036±0.009	−0.095±0.026
D10		−0.007±0.004	(+0.0006±0.003)		−0.019±0.007	−0.057±0.019
D11		(−0.004±0.004)			−0.007±0.005	−0.028±0.011
D12					(−0.002±0.005)	−0.011±0.008

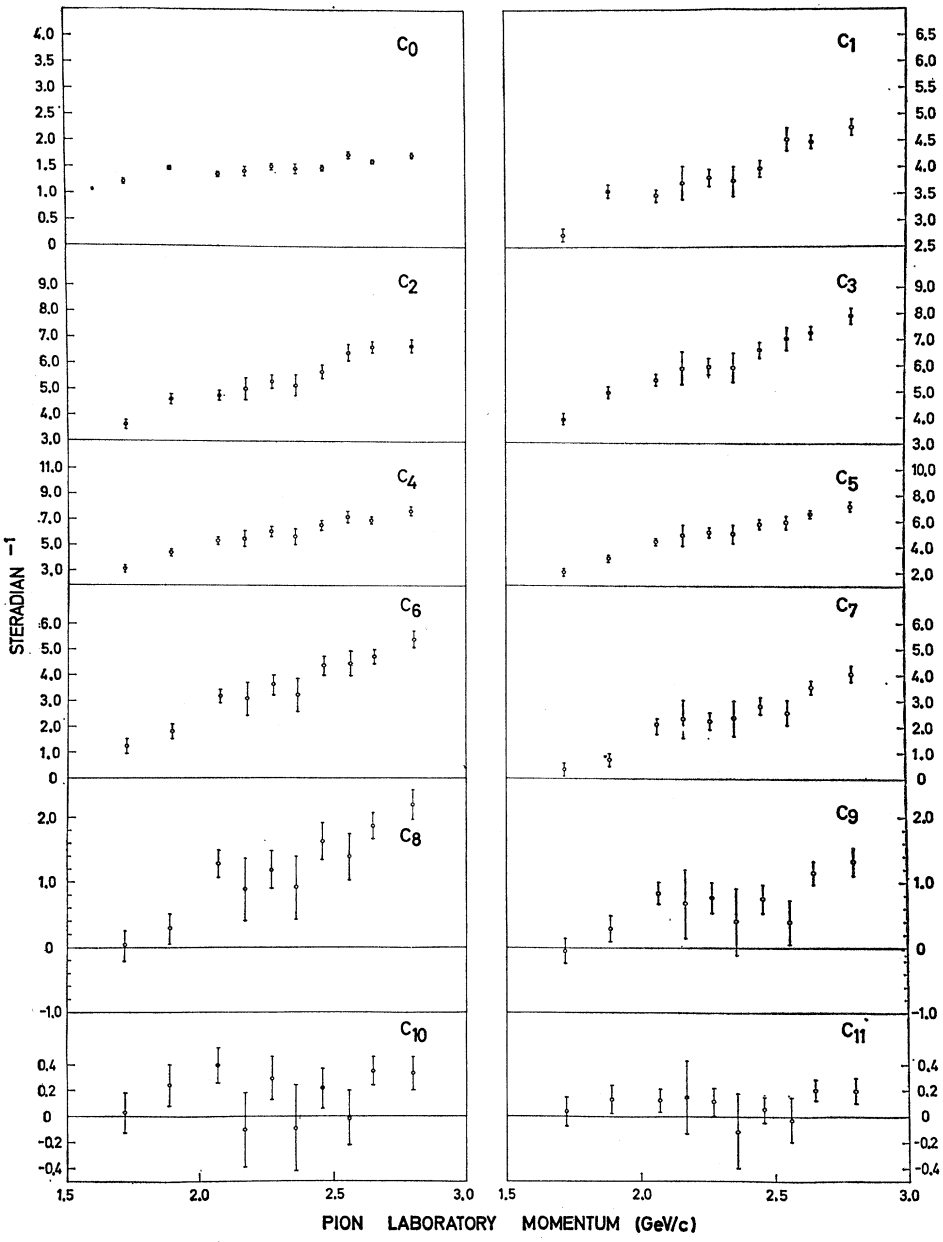

FIG. 3. $\pi^- p$: Legendre polynomial expansion coefficients.

TABLE V. A Coefficients from exponential fit to diffraction-peak data.

Pion lab momentum (GeV/c)	A coefficients, π^+p data ((GeV/c)$^{-2}$)	A coefficients, π^-p data ((GeV/c)$^{-2}$)
1.72	7.75±0.38	7.19±0.68
1.89	6.19±0.40	6.64±0.52
2.07	5.88±0.34	8.38±0.47
2.17	5.25±0.38	8.04±0.61
2.27	5.99±0.45	8.96±0.94
2.36	6.06±0.42	8.84±1.20
2.46	6.53±0.23	7.90±0.63
2.56	6.08±0.28	7.20±0.61
2.65	6.89±0.42	7.59±0.22
2.80	6.44±0.51	7.26±0.43

tabulated by Rosenfeld *et al.*,[15] yields $\delta_l=\frac{1}{4}\pi$, $\frac{1}{2}\pi$, and $\frac{3}{4}\pi$ at the pion momenta 1.85, 2.07, and 2.31 GeV/c, respectively. Since no data at the outer momenta are available, data from the present experiment at 1.89, 2.07, and 2.27 GeV/c have been used. This corresponds to a value of $\Gamma_l\sim 170$ MeV.

The experimental dcs were first fitted to a Legendre polynomial expansion, and the errors shown in Fig. 7 correspond to the errors on the fitted curves.

These results indicate both a dip and secondary maximum in the background term in the region of interest. Similar results were obtained using the data of Esterling *et al.*[16] at pion momenta 1.88, 2.07, and 2.27 GeV/c. $(k^2d\sigma/d\Omega)_b$ from this calculation is also shown in Fig. 7(d).

TABLE VI. Results of two-parameter optical-model fits to π^+p data.

Pion lab momentum (GeV/c)	R (F)	a
1.72	0.91±0.01	0.35±0.01
1.89	0.83±0.01	0.34±0.01
2.07	0.79±0.01	0.35±0.01
2.17	0.83±0.01	0.38±0.01
2.27	0.84±0.01	0.37±0.01
2.36	0.86±0.01	0.42±0.01
2.46	0.87±0.01	0.41±0.01
2.56	0.86±0.01	0.41±0.01
2.65	0.86±0.01	0.42±0.01
2.80	0.86±0.01	0.42±0.01

[15] A. H. Rosenfeld *et al.*, University of California Radiation Laboratory Report No. UCRL-8030, 1967 (unpublished).

[16] R. J. Esterling *et al.*, Report No. EFINS 66-29, 1966 (unpublished).

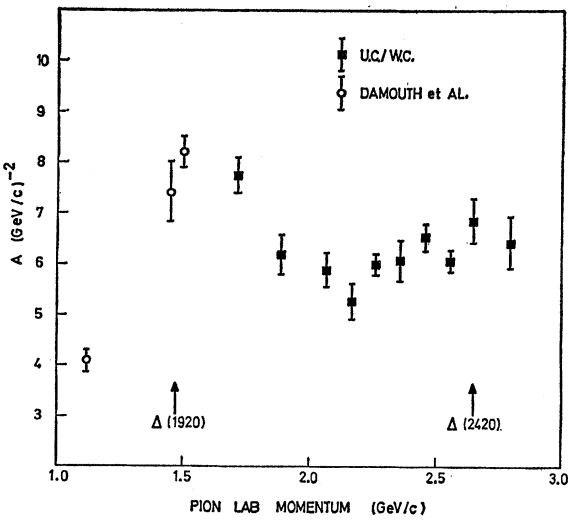

FIG. 4. π^+p: A coefficients from exponential fit to diffraction-peak data.

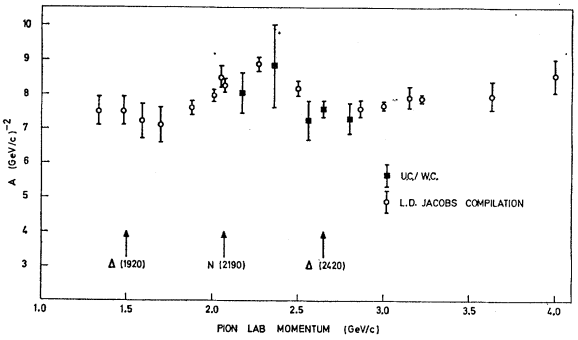

FIG. 5. π^-p: A coefficients from exponential fit to diffraction-peak data.

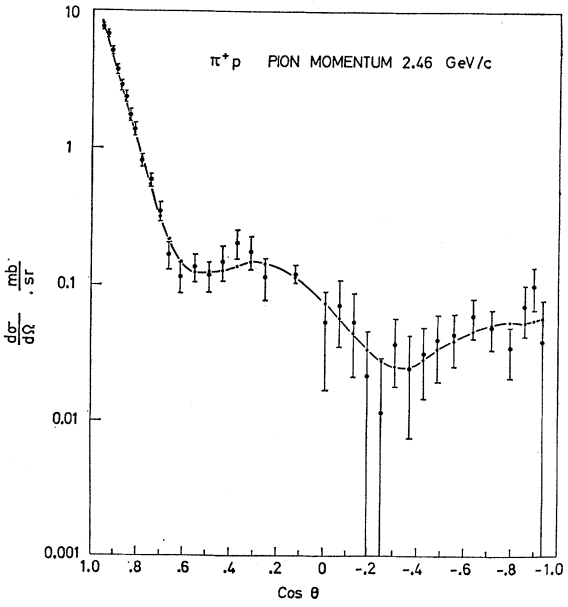

FIG. 6. π^+p: Comparison of empirical partial-wave analysis with experimental data at 2.46 GeV/c.

If data at 1.72, 2.07, and 2.46 GeV/c are used, corresponding to a value of $\Gamma_l \sim 330$ MeV, then agreement with the results of Hoff's analysis, in which the secondary maximum appears predominantly in the interference term, is obtained.

dcs at 1.72, 1.89, and 2.07 GeV/c reconstructed from CERN phase-shift solutions[17] leaving out the $G17$ contribution indicate a dip and secondary maximum structure in the background, as shown in Fig. 8. It is concluded that a more precise knowledge of Γ_l for the $N(2190)$ is required before the results of a calculation based on Eq. (6) could be interpreted as evidence for

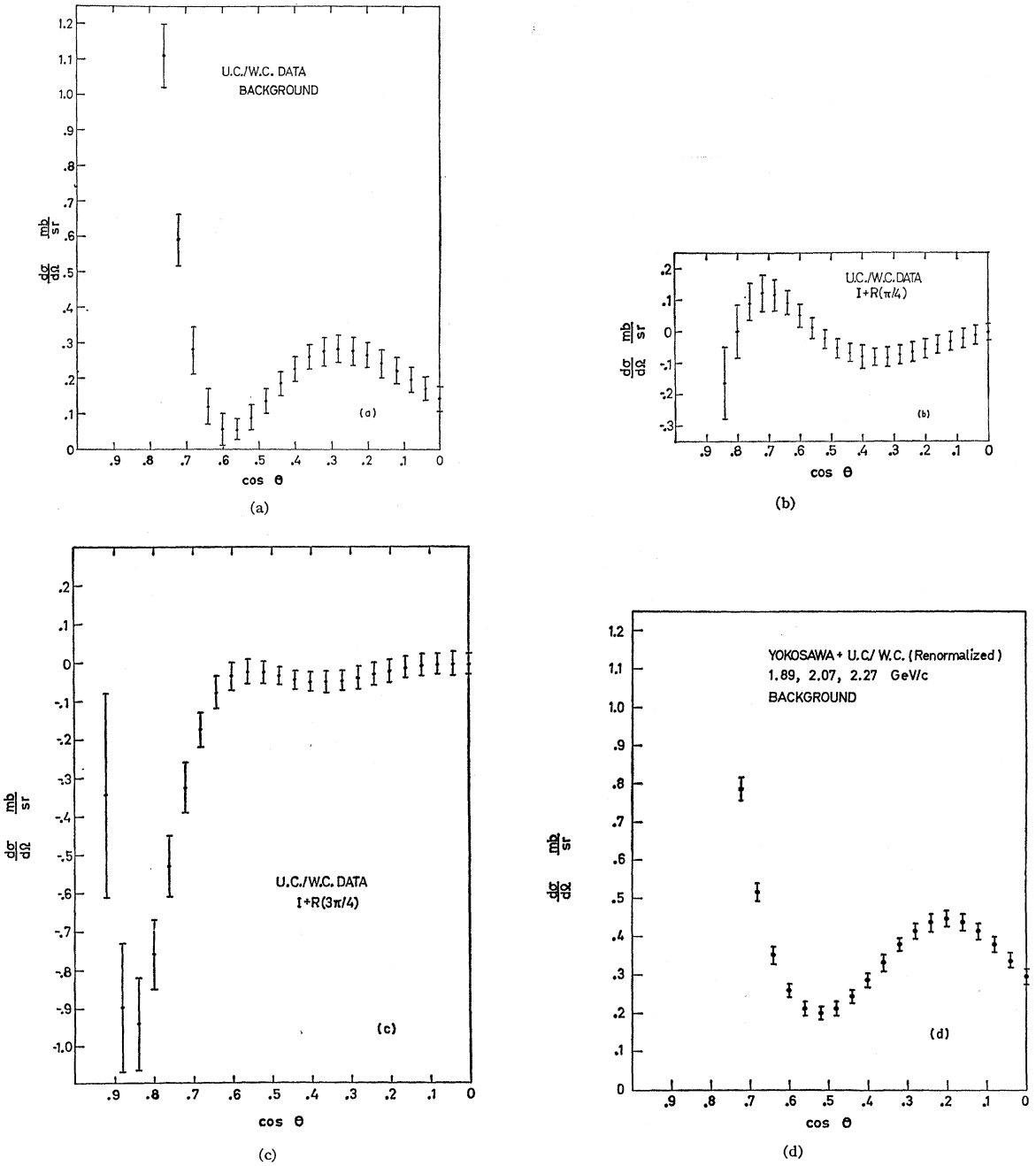

FIG. 7. $\pi^- p$: Background and interference+resonance components of dcs (a), (b), and (c) from data of the present experiment: (a) $[k^2(d\sigma/d\Omega)]_b$, (b) $[k^2(d\sigma/d\Omega)]_{i+r}$ at 1.89 GeV/c, (c) $[k^2(d\sigma/d\Omega)]_{i+r}$ at 2.27 GeV/c, and (d) $[k^2(d\sigma/d\Omega)]_b$ from data of Ref. 16.

[17] A. Donnachie *et al.*, CERN Report No. TH-838, 1967; (unpublished).

TABLE VII. π^+p empirical partial-wave analysis.

Pion lab momentum (GeV/c)	L_{max}	χ^2	a_0	a_1	a_2	a_3	a_4	a_5	a_6	a_7
1.72	4	2.62	1.94±0.02	0.44±0.01	0.38±0.01	0.38±0.01	0.15±0.01			
1.89	5	1.97	1.69±0.02	0.66±0.01	0.38±0.01	0.38±0.01	0.13±0.01	0.06±0.01		
2.07	6	0.92	1.61±0.02	0.66±0.01	0.31±0.01	0.31±0.01	0.15±0.01	0.05±0.01	0.001±0.004	
2.17	6	1.30	1.56±0.03	0.67±0.01	0.28±0.02	0.28±0.02	0.18±0.01	0.07±0.01	0.001±0.009	
2.27	6	1.81	1.53±0.03	0.75±0.01	0.29±0.01	0.29±0.01	0.23±0.01	0.07±0.01	0.04 ±0.10	
2.36	6	0.64	1.54±0.05	0.68±0.02	0.27±0.02	0.27±0.02	0.22±0.02	0.12±0.02	0.006±0.013	
2.46	6	0.70	1.55±0.03	0.72±0.01	0.31±0.01	0.31±0.01	0.23±0.01	0.14±0.01	0.04 ±0.01	
2.56	6	0.97	1.18±0.04	1.0[a]	0.34±0.02	0.34±0.02	0.29±0.02	0.12±0.02	0.07 ±0.02	
2.65	7	0.84	1.51±0.03	0.74±0.02	0.33±0.01	0.33±0.01	0.26±0.01	0.16±0.01	0.06 ±0.01	0.01±0.01
2.80	7	1.12	1.59±0.03	0.76±0.02	0.37±0.01	0.37±0.01	0.24±0.01	0.19±0.01	0.08 ±0.01	0.03±0.01

[a] Parameter value equal to constraint limit.

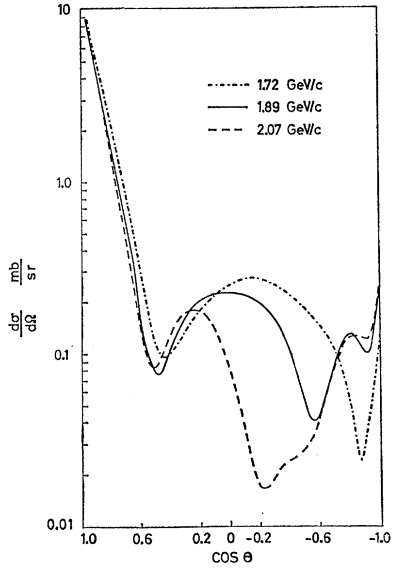

FIG. 8. π^-p: dcs at 1.72, 1.89, and 2.07 GeV/c reconstructed from phase-shift solution, omitting the $G17$ wave.

the phenomenon of double counting in this energy region.[18]

ACKNOWLEDGMENTS

We wish to thank the Science Research Council for financing this work. We also thank the staff of the Rutherford High Energy Laboratory, the University of London Computing Centre, and the University College London Computing Centre for their cooperation. The contributions of the technical staff and data reduction teams of University College London, and Westfield College, London are gratefully acknowledged. In conclusion, five of us (T. F. B., R. W. D., K. M. P., J. A. S., and T. P. S.) wish to thank the Science Research Council for financial assistance in the form of maintainance grants.

[18] R. Dolen, D. Horn and C. Schmid, CALTEC Report No. CALT-63-143 (unpublished); Phys. Rev. Letters **19**, 402 (1965).